Ultra-wideband Frequency Analysis: State-of-the-art, Measurements and Modeling

*Gonzalo Llano, Juan Reig, Lorenzo Rubio and Alexis P. García**
Instituto de Telecomunicaciones y Aplicaciones Multimedia (iTEAM)
Universidad Politécnica de Valencia
Building 8G, access D, Camino de Vera s/n 46022 Valencia (SPAIN)
**Ilmenau University of Technology*
Corresponding author: jreigp@dcom.upv.es or lrubio@dcom.upv.es

Abstract

This paper presents a tutorial overview of ultra-wideband (UWB) propagation models. The channels models IEEE 802.15.3a y IEEE 802.15.4a are revised and examined. Subsequently, the UWB channel in the frequency domain is analyzed. Results of the amplitude statistics in this domain and of the correlation coefficient between subcarriers in a MB-OFDM UWB system are obtained. In addition, the UWB channel energy in function of the bandwidth is analyzed from a measurement campaign indoor of the channel impulse response and a theoretic model for the fade depth and fading margin of the channel energy is proposed in accordance to the parameters of the IEEE 802.15.4a UWB channel model. This investigation is based on a measurement campaign carried out in a typical laboratory environment in the 3.1-10.6 GHz band in accordance to the UWB frequency range. The model considers line-of-sight (LOS) and non-line-of-sight (NLOS) conditions. This model is very useful to determine the optimal operation bandwidth with a desired quality of service in wireless systems.

Keywords: UBW, OFDM, lognormal, Nakagami-m fading, fade depth, fading margin.

1.Introduction

Ultra wideband (UWB) transmission systems are characterized with either a fractional bandwidth of more that 20 %, or a large absolute bandwidth (> 500 MHz) and for a very low power spectral density (–41.25dBm/MHz, equivalent to 75nW/MHz) [1]. For this reason, UWB systems are emerging as the best solution for high speed short range indoor wireless communication and sensor networks, with applications in home networking, high-quality multimedia content delivery, radars systems of high accuracy, etc. UWB has many attractive properties, including low interference to and from other wireless systems, easier wall and floor penetration, and inherent security due to its low probability interception/detection (LPI/D). Two of the most promising applications of UWB are High Data Rate Wireless Personal Area Network (HDR-WPAN), and sensor networks, where the good ranging and geo-location capabilities of UWB are particularly useful and of interest for military applications [2]. Three types of UWB systems are defined by the Federal Communications Commission in United States: imaging systems, communication, measurement, and vehicular radar Systems. Currently the United States permits operation of UWB devices. In Europe a standardization mandate was forwarded to CEN/CENELEC/ETSI for harmonized standards covering UWB equipment [3], and regulatory efforts are studied by Japan [2]. In order to deploy UWB systems which carry out all those potentials, we need to analyze UWB propagation and the channel properties arising from this propagation. Given the large bandwidth (7.5 GHz) authorized for UWB, the conventional channel models developed for narrowband transmissions are inadequate in UWB [2]. This paper is organized as follows: Section 2 describes the statistical characterization of the channel models IEEE 802.15.3a and IEEE 802.15.4a. In section 3, we present the results and simulations for the UWB channel IEEE 802.15.3a in the frequency domain. Section 4 investigates analytical results of the channel energy as a function of the bandwidth for the IEEE 802.15.4a model. Furthermore we analyze measurements for an UWB indoor channel, and finally section 5 concludes this paper.

2. UWB statistical channel model

The 802.15.3a TG has proposed a channel model for HDR-WPAN applications [4] and the 802.15.4a TG a channel model for evaluation of the IEEE 802.15.4a standard [5]. This model can be used in indoor and outdoor environments with longer operating range (i.e., >10 m in indoor and up to few hundred meters for outdoor environments) and lower data rate transmission (between 1 kb/s and several Mb/s).

The multipath arrival times are ran-dom process based on the Poisson distribution. The small scale amplitude follows a lognormal or Nakagami-m distribution.

2.1 IEEE 802.15.3a channel model

The IEEE 802.15.3a UWB-OFDM channel for UWB communications systems defines a modified Saleh-Valenzuela (SV) [6] model to describe the arrival time of clusters (multipath components, MPC, which arrive from a same scatter) and MPC at the receiver after multipath propagation. To characterize the UWB channel for HDR-WPAN applications, three indoor channel models were evaluated by the 802.15.3a TG [4]: the Rayleigh tap delay line model, the SV [6] and the *Λ-K* [7].

The SV and *Λ-K* models use a Poisson distribution in order to model the arrival time of MPC. Nevertheless, the SV model is unique in its approach of modeling the arrival time in cluster as well as MPC within a cluster. The SV model defines that the multipath arrival times are random process based in Poisson distributions. Therefore the interarrival time of MPC is exponentially distributed, and defines also four parameters to describe the channel: The cluster arrival rate *(Λ),* the path arrival rate *(λ)* within a cluster, the cluster decay time constant *(η),* and the path time constant *(γ)*.

The principle of a SV channel is shown in the Fig. 1. In this model, the small scale amplitude fading statistics follow a Rayleigh distribution and the power is defined by the cluster and ray decay factors. However, measurements in UWB channels indicated that the small scale amplitude statistics follow a lognormal or Nakagami-*m* distribution and the power of the clusters and ray decays over time; this was modeled as an exponentially decaying power profile with increasing delay from the first path. Based on these results, the SV model was modified for IEEE TG3a, defining the channel impulse response (CIR), denoted by *h(τ),* as [4]

$$h(\tau)=\sum_{l=1}^{L_c}\sum_{k=1}^{L_r}\xi_l\beta_{k,l}e^{j\varphi_{k,l}}\delta\left(\tau-T_l-\tau_{k,l}\right) \tag{1}$$

where l represents the cluster index and k the MPC index within a lth cluster; L_c and L_r are the number of clusters and MPC, respectively; T_l is the arrival time of the lth cluster; and $\tau_{k,l}$ is the arrival time of the kth component inside the lth cluster. ξ_l is the amplitude of the lth cluster, $\beta_{k,l}$ is the amplitude of the kth path inside the lth cluster, and $\varphi_{k,l}$ is the phase of the path. The mean power of the kth path is given by

$$\Omega_{k,l}=E\left[\left|\xi_l\beta_{k,l}\right|^2\right]=\Omega_0\exp\left(-T_l/\eta\right)\exp\left(-\tau_{k,l}/\gamma\right) \tag{2}$$

where Ω_0 is the mean power of the first path inside the first cluster. The amplitudes of the contributions $|\xi_l\beta_{k,l}|$ are mutually independent random variables (RVs) and their phases $\varphi_{k,l}$ are uniformly distributed from 0 to 2π. The module of the amplitude of the paths follows a lognormal distribution, given by

$$\left|\xi_l\beta_{k,l}\right|=10^{\left(\mu_{k,l}+n_1+n_2\right)/20}\rightarrow 20\log\left(\xi_l\beta_{k,l}\right)\sim N\left(\mu_{k,l},\sigma_c^2+\sigma_r^2\right) \tag{3}$$

where n_1 and n_2 are independent normal RV with zero mean and standard deviations σ_c and σ_r, given by $n_1 \sim N(0, \sigma_c)$ and $n_2 \sim N(0, \sigma_r)$ and correspond to the fading on each cluster and path respectively; and $N(a, b)$ represents a Gaussian distribution with mean a and standard deviation b. The mean for the lognormal distribution of $|\xi_l\beta_{k,l}|$ can be obtained from (2) and (3) as

$$\mu_{k,l}=\frac{10\ln\left(\Omega_0\right)-10T_l/\eta-10\tau_{k,l}/\gamma}{\ln(10)}-\frac{\left(\sigma_c^2+\sigma_r^2\right)\ln(10)}{20}. \tag{4}$$

The distribution of the cluster arrival time and ray arrival time is exponential whose probability density function (PDF) is given by

$$p_T\left(T_l\left|T_{l-1}\right.\right)=\Lambda\exp\left[-\Lambda\left(T_l-T_{l-1}\right)\right],\ l>0,$$
$$p_\tau\left(\tau_{k,l}\left|\tau_{(k-1),l}\right.\right)=\lambda\exp\left[-\lambda\left(\tau_{k,l}-\tau_{(k-1),l}\right)\right],\ k>0 \tag{5}$$

More details of the model parameters can be found in [4].

IEEE 802.15.4a channel model

This model was developed by the IEEE 802.15.4a standardization group for UWB systems ranging with low rates transmission [5]. The CIR is modeled for the IEEE 802.15.4a by a generalized SV model, where the number of clusters L_c is a Poisson distributed RV; the mean number of clusters $\overline{L_c}$, is a parameter of the model and its PDF is given by [5]

$$p_{L_c}\left(L_c\right)=\frac{\left(\overline{L_c}\right)^{L_c}}{L_c!}\exp\left(-\overline{L_c}\right),\ L_c>0, \tag{6}$$

Just like in the IEEE 802.15.3a channel model, the interarrival times of the cluster in the IEEE 802.15.4a channel are Poisson processes given by (5). Due to the discrepancy in the fitting for the indoor residential, and indoor and outdoor office environments [5], the 802.15.4a TG proposes to model ray arrival times with mixtures of two Poisson processes as follows

$$p_\tau\left(\tau_{k,l}\left|\tau_{(k-1),l}\right.\right)=\beta\lambda_1\exp\left[-\lambda_1\left(\tau_{k,l}-\tau_{(k-1),l}\right)\right]$$
$$+\left(1-\beta\right)\lambda_2\exp\left[-\lambda_2\left(\tau_{k,l}-\tau_{(k-1),l}\right)\right],\ k>0, \tag{7}$$

where β is the mixture probability, λ_1 and λ_2 are the ray arrival rates. The power delay profile (PDP) is exponentially distributed within each cluster and is given by

$$\Omega_{k,l} = E\left[\left|\alpha_{k,l}\right|^2\right] = \Omega_l \frac{1}{\gamma_l\left[(1-\beta)\lambda_1 + \beta\lambda_2 + 1\right]} \exp\left(-\tau_{k,l}/\gamma_l\right),$$

(8)

where Ω_l is the integrated mean energy of the lth cluster, and γ_l is the intra-cluster decay time constant.

The mean energy Ω_l of the lth cluster follows an exponential decay, and in agreement [5]

$$10\log\left(\Omega_l\right) = 10\log\left[\exp\left(-T_l/\eta\right)\right] + M_{cluster},$$

(9)

where T_l is the arrival time of the cluster given by (5). $M_{cluster}$ is a RV Gaussian distributed with standard deviation $\sigma_{cluster}$. The cluster decay rates γ_l depend linearly on the arrival time of the cluster and is expressed as $\gamma_l = kT_l + \gamma_0$, where k and γ_0 are parameters of the model. The small scale fading for the multipath gain magnitude $\alpha_{k,l}$, is modeled as a Nakagami-m distribution and is given by [8]

$$p_{\alpha_{k,l}}\left(\alpha_{k,l}\right) = \frac{2}{\Gamma(m)}\left(\frac{m}{\Omega_{k,l}}\right)^m \alpha_{k,l}^{2m-1} \exp\left(-\frac{m}{\Omega_{k,l}}\alpha_{k,l}^2\right), \quad m \geq 0.5,$$

(10)

where m is the fading parameter of the kth path, $\Gamma(\cdot)$ is the gamma function, and $\Omega_{k,l}$ is average power of the kth path given by (8). The m parameter is modeled as a lognormal distributed RV, whose logarithm has a mean μ_m and standard deviation σ_m given by [5]

$$\mu_m(\tau) = m_0 - k_m(\tau); \qquad \sigma_m(\tau) = \hat{m}_0 - \hat{k}_m(\tau)$$

(11)

where $m_0, k_m, \hat{m}_0, \hat{k}_m$, are parameters of the model.

Frequency Domain Channel Response

The study of the UWB channel in the frequency can be of great interest to analyze the performance of the MB-OFDM UWB system concerning to the channel estimation, and bit and symbol error analysis. Moreover, an accurate model in frequency of the UWB channel is required to design adaptive modulation techniques which increase the channel capacity. In the frequency domain we obtain a Nakagami-m approximate distribution of subcarriers envelope for the IEEE 802.15.3a UWB model. The correlation coefficient between a couple of subcarriers amplitudes is calculated analytically. Hence, we will calculate the Fourier transform (FT) of the CIR given by (1). We will show that if the amplitude $|\zeta_l\beta_{k,l}|$ of each UWB channel contribution is modeled as a log-normal RV and the number of MPC is high, the magnitude of the ith subcarrier can be approximated by a Nakagami-m RV. The FT of the CIR and denoted by $H(f)$ is expressed as

$$H(f) = \sum_{l=1}^{L_c}\sum_{k=1}^{L_r} \xi_l \beta_{k,l} \exp\left[-j\left(2\pi f\left(T_l + \tau_{k,l}\right) - \varphi_{k,l}\right)\right].$$

(12)

Average power and fading parameter

The average power of the ith subcarrier in the frequency domain is obtained as

$$\Omega_{eq}^i = \sum_{l=0}^{L_c-1}\sum_{k=0}^{L_r-1} \Omega_{k,l} = \sum_{l=0}^{L_c-1}\sum_{k=0}^{L_r-1} \Omega_0 \exp\left[-\left(\frac{T_l}{\eta} + \frac{\tau_{k,l}}{\gamma}\right)\right],$$

(13)

The fading parameter m_{eq}^i of the ith subcarrier can be calculated as

$$m_{eq}^i = \frac{\left(\sum_{l=0}^{L_c-1}\sum_{k=0}^{L_r-1} \Omega_{k,l}\right)^2}{A\sum_{l=0}^{L_c-1}\sum_{k=0}^{L_r-1} \Omega_{k,l}^2 + \sum_{l=0}^{L_c-1}\sum_{k=0}^{L_r-1}\sum_{n=0}^{L_c-1}\sum_{m=0}^{L_r-1} \Omega_{m,n}\Omega_{k,l}},$$

(14)

with $A = \exp\left(4\sigma_{np}^2\right) - 2$ and σ_{np} the standard deviation of the lognormal fading, in nepers units, given by

$$\sigma_{np} = \frac{\ln(10)}{20}\sqrt{\sigma_c^2 + \sigma_r^2},$$

(15)

where σ_c and σ_r are the standard deviations in dB units of clusters and rays, respectively. Fig. 2 shows the comparison of the amplitude $|H(f_i)|$ cumulative distribution function (CDF) between simulated data and the Nakagami-m approximation, where Ω_{eq} and m_{eq} are calculated from (13) and (14). 8 clusters and 12 rays by cluster were assumed in simulations. The rest of parameters used in Fig.2 were: $\sigma_c = \sigma_r = 3.4$ dB, $\eta = 24$, $\gamma = 12$ and $\Omega_0 = 1$. From Fig. 2, it can be observed that the Nakagami-m approximation and simulation curves are very similar and these results show

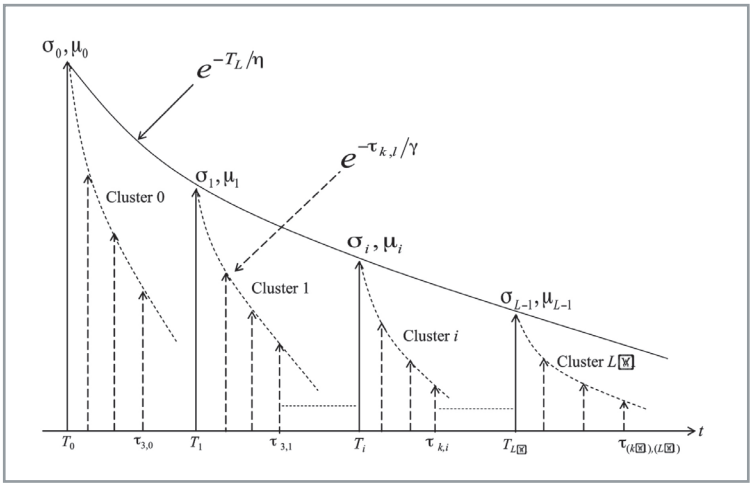

Figure 1. *Principle of the Saleh-Valenzuela channel model*

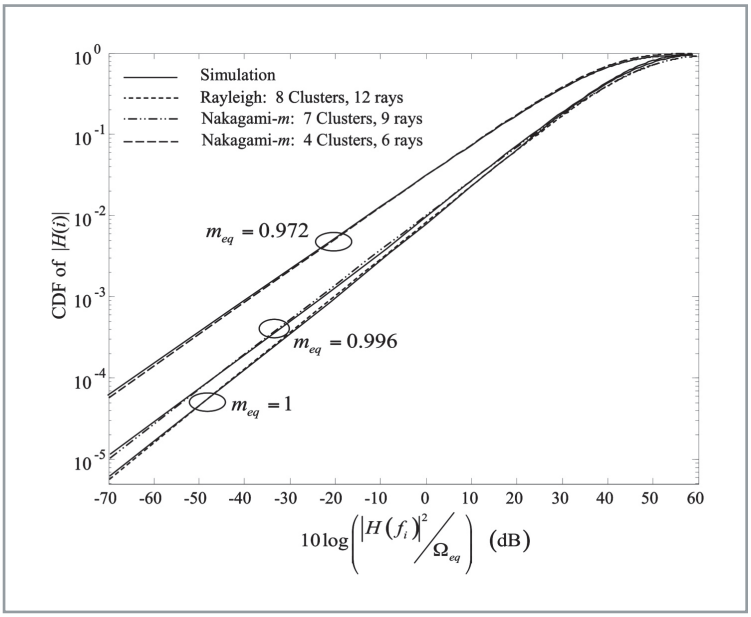

Figure 2. *Cumulative distribution function of the normalized channel frequency amplitude, in logarithmic units, for several UWB channels*

that for a UWB channel with Nakagami-*m* fading and independents MPC: a) the magnitude of the channel response frequency at each frequency bin is approximately Nakagami-*m* distributed with parameters defined by (13) and (14); and b) If the MPC number is higher that 96 (number of rays multiplied by number of clusters) then the relative error in the m_{eq} is less than 0.1% with respect to $m_{eq}=1$. Note that $|H(f_i)|$ becomes Rayleigh for a sufficiently high number of MPC (typical environment in UWB channels). For instance, if the MPC number is higher than 63 contributions then the difference of the CDF for 10^{-3} between the simulated distribution and the Rayleigh distribution is less than 2 dB.

Correlation coefficient

The correlation coefficient, $\rho_{i,j}$, between the *i*th and the *j*th subcarriers is defined as

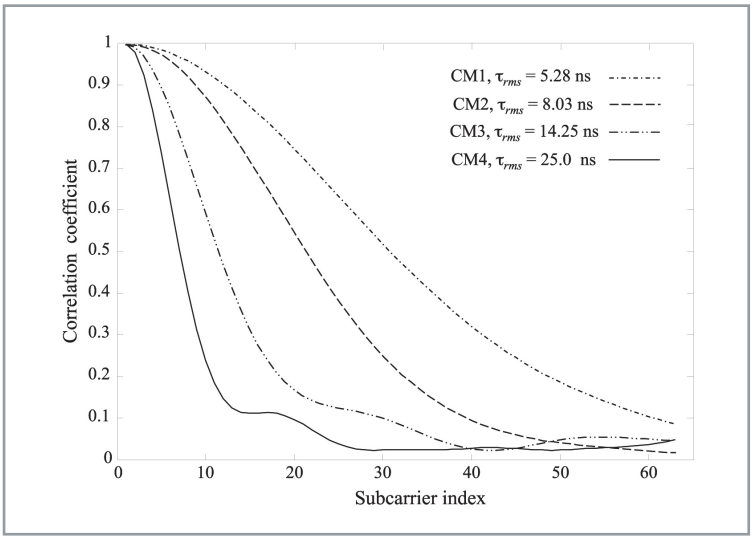

Figure 3. *Correlation coefficient as a function of the subcarrier order with respect to the first subcarrier position*

$$\rho_{ij}=\frac{\mathrm{cov}\left(\alpha_i^2,\alpha_j^2\right)}{\sqrt{\mathrm{var}\left(\alpha_i^2\right)\mathrm{var}\left(\alpha_j^2\right)}}=\frac{E\left[\alpha_i^2\alpha_j^2\right]-E\left[\alpha_i^2\right]E\left[\alpha_j^2\right]}{\sqrt{\mathrm{var}\left(\alpha_i^2\right)\mathrm{var}\left(\alpha_j^2\right)}},\tag{16}$$

where var $(\cdot)$ is the variance of the RV given by [8] as

$$\mathrm{var}\left(\alpha_i^2\right)=\mathrm{var}\left[\left|H(f_i)\right|^2\right]=\frac{\Omega_{eq}^2}{m_{eq}}.\tag{17}$$

From (13), (14) and (17), it can be easily obtained a closed form expression of the correlation coefficient in the UWB channel in the frequency domain as

$$\rho_{ij}=\frac{A\sum_{l=1}^{L_c}\sum_{k=1}^{L_r}\Omega_{k,l}^2+\sum_{l=1}^{L_c}\sum_{k=1}^{L_r}\sum_{n=1}^{L_c}\sum_{m=1}^{L_r}\Omega_{m,n}\Omega_{k,l}\cos B_{l,n}^{k,m}}{A\sum_{l=1}^{L_c}\sum_{k=1}^{L_r}\Omega_{k,l}^2+\sum_{l=1}^{L_c}\sum_{k=1}^{L_r}\sum_{n=1}^{L_c}\sum_{m=1}^{L_r}\Omega_{m,n}\Omega_{k,l}},\tag{18}$$

where

$$B_{l,n}^{k,m}=\frac{2\pi}{T_s}\left(\left(T_l+\tau_{k,l}\right)-\left(T_n+\tau_{m,n}\right)\right)(i-j)$$

Fig. 3 shows the correlation coefficient as a function of the UWB channel delay spread, τ_{rms}, for four channel scenarios of the channel model of the IEEE 802.15.3a: CM1(τ_{rms}=5.28 ns) CM2(τ_{rms}=8.03 ns), CM3(τ_{rms}=14.25 ns), and CM4(τ_{rms}=25 ns). From this figure, we can observe a high dependence of the correlation coefficient between a couple of subcarriers on the delay spread. The parameters used in the simulations are given by [5].

4. The Energy in UWB Channel

In this section the fade depth and the fading margin for the IEEE 802.4a channel model are analyzed. We investigate analytically the relation between the fade depth, and the fading margin with channel bandwidth (7.5 GHz). To the author's knowledge these results are novel in the literature of UWB energy modeling especially using the IEEE 802.15.4a model.

4.1. Energy Measurements

Indoor wideband channel measurements were carried out at the high frequency communications laboratory of the Telecommunications School at the Polytechnic University of Valencia. The complex channel transfer function, denoted by, $H(f)$ was measured in the frequency domain using a vector network analyser (VNA).

Biconical omnidirectional wideband antennas with flat frequency response, at the transmitter and the receiver, very low attenuation cables and a wideband low noise amplifier at the receiver

complete the measuring equipment. The transmitting and the receiving antennas were placed at a height of 1.5 m above the ground. The receiving antenna was set up over a precise linear positioning robotic system emulating a 4x4 element squared grid with 4.38 cm inter-element separation (wavelength at 6.85 GHz) to allow sufficient decorrelation. For each position of the squared grid, 300 complex channel transfer functions were measured over a bandwidth of 7.5 GHz (SPAN in the VNA) with 6.85 GHz as a central frequency (f_c), in order to cover all the UWB frequency range (3.1 GHz - 10.6 GHz). Each complex channel transfer function was measured with a frequency resolution of 375 kHz (20,001 spectrum samples). A total of six locations were measured in line-of-sight (LOS) condition and four locations in non-line-of-sight (NLOS), where the receiving antenna was placed in an adjacent room.

The maximum distance between the transmitter and the receiver positions was 5 m and 12 m in LOS and NLOS conditions, respectively. For each location of the squared grid, the individual channel transfer functions were normalised with respect to the mean channel energy in order to eliminate the path-loss, since the large-scale propagation effect is not of interest here. The measurements were carried out at nights, in absence of people, guaranteeing stationary channel conditions.

The measured complex channel transfer function, $H(f)$, with bandwidth of 7.5 GHz and f_c = 6.85 GHz, is partitioned in N_b subbands of bandwidth Δf centred at f_c. The channel energy $\varepsilon_{\Delta f}$, of each subbands $H_b(f)$ with $b = 1, 2, \ldots, N_b$, can be calculated by the squared integration of the frequency domain coefficients of $H_b(f)$, i.e. $\varepsilon_{\Delta f} = \int_{f_1}^{f_2} |H_b(f)|^2 \, df$, where $f_1 = f_c - \Delta f/2$ and $f_2 = f_c + \Delta f/2$.

The fade depth, F, is a measure of the variation in the channel energy about its local mean due to small-scale fading. It can be evaluated in terms of standard deviation, σ, of the channel energy expressed in logarithmical units, dB. We can define F to span the $s\sigma$ range of E_b variations, denoted by $F_{s\sigma}$, thereby the number of standard deviations considered in the variation of the channel energy is s. Then, the fade depth associated to a channel bandwidth Δf can be derived from the measurements. Fig. 4 and Fig 5 show the fade depth averaged across the channel ensemble, $F_{3\sigma}$, expressed as a function of Δf in LOS and NLOS condition. From the measured data, $F_{3\sigma}$ in LOS conditions is found to be about 15.4 dB for a bandwidth channel of 6 MHz, decreasing to about 2 dB for a bandwidth channel of 1 GHz and 1 dB for a bandwidth channel of 7.5 GHz. In NLOS conditions, $F_{3\sigma}$ is approximately 14 dB for a bandwidth channel of 6 MHz, decreasing to around 3 dB for a bandwidth channel of 1 GHz and 1.5 dB for a bandwidth channel of 7.5 GHz.

4.2. Energy Analysis

In the channel model proposed by the 802.15.4a TG, the amplitude $\alpha_{k,l} = |\xi \beta_{k,l}|$ of each MPC follows a Nakagami-m distribution [5], the CIR $h(\tau)$ is given by (1) and its Fourier transform by (12).

The UWB channel energy in watts inside the bandwidth $\Delta f(HZ) = f_2 - f_1$ is calculated as

$$\varepsilon_{\Delta f}(\mathrm{W}) = \int_{f_1}^{f_2} \left| H(f) \right|^2 df, \tag{19}$$

where $|H(f)|$ is the magnitude of the ith bin in frequency. After some mathematical operations, the energy of the UWB channel is given by

$$\varepsilon_{\Delta f}(\mathrm{W}) = \Delta f \sum_{l=1}^{L_c} \sum_{k=1}^{L_r} \alpha_{k,l}^2 + \frac{1}{\pi} \sum_{l=1}^{L_c} \sum_{\substack{k=1 \\ k \neq l}}^{L_r} \sum_{n=1}^{L_c} \sum_{\substack{m=1 \\ m \neq n}}^{L_r} \frac{\alpha_{k,l} \alpha_{m,n}}{(T_l + \tau_{k,l}) - (T_n + \tau_{m,n})}$$
$$\cdot \left(\sin\left[2\pi f_2 \left((T_l + \tau_{k,l}) - (T_n + \tau_{m,n}) \right) + (\varphi_{k,l} - \varphi_{m,n}) \right] \right.$$
$$\left. - \sin\left[2\pi f_1 \left((T_l + \tau_{k,l}) - (T_n + \tau_{m,n}) \right) + (\varphi_{k,l} - \varphi_{m,n}) \right] \right) \tag{20}$$

The mean energy of the channel can be calculated as

$$E\left[\varepsilon_{\Delta f}(\mathrm{W}) \right] = \Delta f \sum_{l=1}^{L_c} \sum_{k=1}^{L_r} E\left[\alpha_{k,l}^2 \right] = \Delta f \sum_{l=1}^{L_c} \sum_{k=1}^{L_r} \Omega_{k,l}, \tag{21}$$

where $\Omega_{k,l}$ is the average power of each UWB

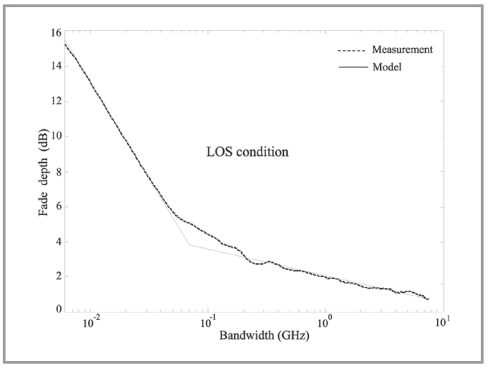

Figure 4. *Fade depth in terms of the channel bandwidth in LOS condition.*

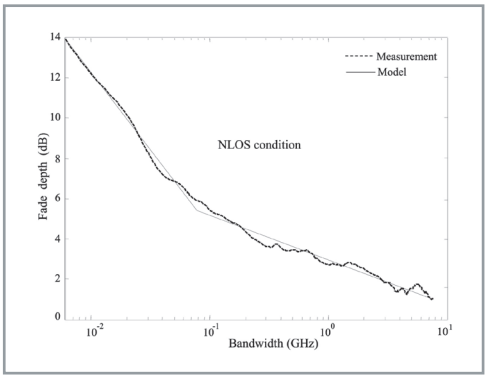

Figure 5. *Fade depth in terms of the channel bandwidth in NLOS condition.*

channel contribution. Now, we investigate the variation of the channel energy with bandwidth, evaluating the fade depth and fading margin.

4.2.1. Fade Depth

Statistically the fade depth is related with standard deviation, σ_{Φ}, of the channel energy expressed in logarithmic units, $\Phi(dBW)=10log[\varepsilon_{\Delta f}(W)]$. If we assume that the energy given by (20) is approximated by a gamma distribution, the variance and the standard deviation of the energy Φ(dBW) are given by

$$\mathrm{var}_{\Phi}(\mathrm{dB})=\left[\frac{10}{\ln(10)}\right]^2\psi'(m_{eq});\qquad \sigma_{\Phi}(\mathrm{dB})=\frac{10}{\ln(10)}\sqrt{\psi'(m_{eq})}\,. \tag{22}$$

where

$$\psi'(a)=\frac{\partial^2}{\partial a^2}\left\{\ln\left[\Gamma(a)\right]\right\}$$

is the trigamma function [9, (6.4.1)]. In order to evaluation the fade depth, a range of systems performance levels is defined as $s = \{1, 2, 3\}$. The fade depth, $F_{s\sigma}$, is calculated analytically as

$$F_{s\sigma}=\frac{10s}{\ln(10)}\sqrt{\psi'(m_{eq})}\,. \tag{23}$$

To evaluate (23) we need to obtain the fading parameter m_{eq} given by

$$m_{eq}=\frac{\left(E\left[\varepsilon_{\Delta f}\right]\right)^2}{E\left[\varepsilon_{\Delta f}^2\right]-\left(E\left[\varepsilon_{\Delta f}\right]\right)^2}, \tag{24}$$

resulting

$$m_{eq}^{i}=\frac{\left(\Delta f\sum_{l=1}^{L_r}\sum_{k=1}^{L_t}\Omega_{k,l}\right)^2}{(\Delta f)^2\sum_{l=1}^{L_r}\sum_{k=1}^{L_t}\frac{\Omega_{k,l}^2}{m_{k,l}}+\frac{1}{2\pi^2}\sum_{l=1}^{L_r}\sum_{\substack{k=1\\k\neq l}}^{L_t}\sum_{n=1}^{L_r}\sum_{\substack{m=1\\m\neq n}}^{L_t}\frac{\Omega_{k,l}\Omega_{m,n}}{\left[\left(T_l+\tau_{k,l}\right)-\left(T_n+\tau_{m,n}\right)\right]^2}\times D_{l,n}^{k,m}}. \tag{25}$$

where

$$D_{l,n}^{k,m}=\sin^2\left\{\pi\left[\left(T_l+\tau_{k,l}\right)-\left(T_n+\tau_{m,n}\right)\right]\Delta f\right\}$$

Fig. 6 shows that the analytical approximation of the fade depth in a UWB channel IEEE 802.15.4a given by (23) and the comparison with the simulation curves. It can be observed that the simulation curves and the approximation results are very similar, which is in agreement with our assumption that the channel energy follows a gamma distribution. These curves also show that for channels whose bandwidths (Δf) between 100 kHz and 1 MHz, their fade depth is approximately constant, and falls linearly with Δf from 3 MHz to 30 MHz, approximately. $F_{s\sigma}$ curves appear to converge asymptotically to 2 dB from approximately 1.5 GHz. The cluster number is given by (7) and 30 rays by cluster were used in the simulations. The rest of parameters correspond to an indoor residential environment [5].

4.2.2. Fading Margin

The mean energy, fade depth and fading margin are channel parameters used in wireless system design. The fade depth determines the required fade margin and link budget for acceptably low system outage probability [10]. The fading margin, M_F, can be expressed as

$$M_F\,(dB)=E[\Phi(BW)]-\Phi p(dBW) \tag{26}$$

where $\Phi(dBW)$ is the channel energy in dBW, and $\Phi_p(dBW)$ is the energy not exceeded with a probability P (%). The mean of the channel energy, can be calculated as

$$E\left[\Phi(\mathrm{dBW})\right]=\frac{10}{\ln(10)}\psi\left(m_{eq}\right)-10\log\left(\frac{m_{eq}}{\Omega_{eq}}\right). \tag{27}$$

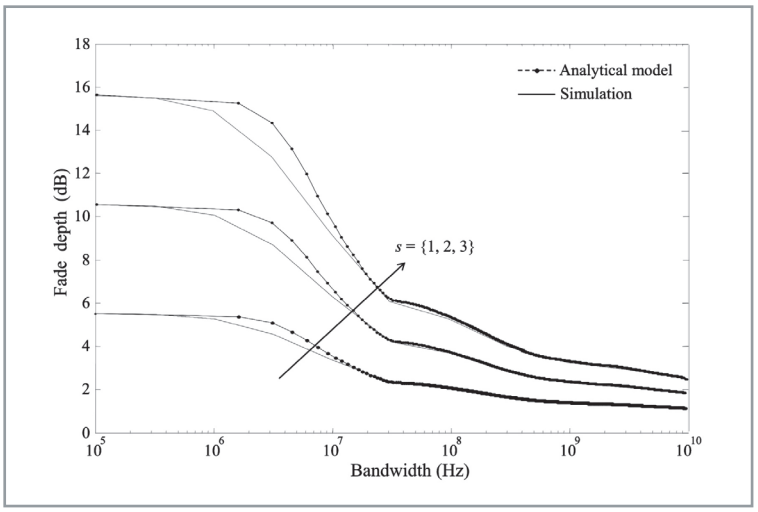

Figure 6. *Fade depth of the UWB Channel IEEE 802.15.4a*

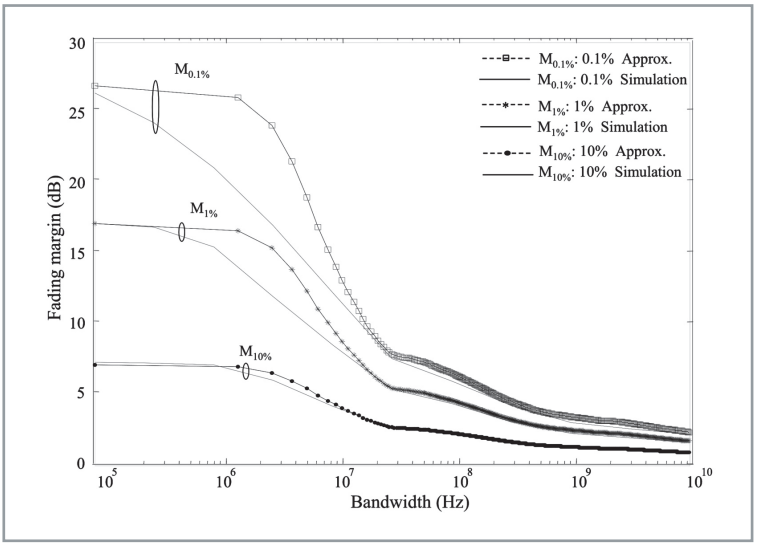

Figure 7. *Fading margin of the UWB Channel IEEE 802.15.4a*

where

$$\psi(a)=\frac{\partial}{\partial a}\left\{\ln\left[\Gamma(a)\right]\right\}$$

is the digamma function [9, (6.3.1)]. $\Phi_p(dBW)$ after some operations is given by

$$\Phi_p(\mathrm{dBW})=10\log\left(\frac{\Omega_{eq}}{m_{eq}}\right)+10\log\left[Q^{-1}\left(m_{eq},\frac{100-P}{100}\right)\right],$$

(28)

where Q^{-1} is the inverse of the regularized incomplete gamma function [11, (06.12.02.0001.01)]. Substituting (27) and (28) in (26), it can be easily to obtain a closed form expression for the fading margin in the frequency domain given by

$$M_F(\mathrm{dB})=\frac{10}{\ln(10)}\psi(m_{eq})-10\log\left[Q^{-1}\left(m_{eq},\frac{100-P}{100}\right)\right].$$

(29)

where m_{eq}, is defined in (25). Fig. 7 shows the fading margin for the UWB channel as a function of the bandwidth for several probabilities $P=0.1\ \%$, 1 % and 10 %. The curve of the analytical approximation for $P=10\ \%$ shows a good agreement with the simulation. For lower probabilities, the gamma approximation of the energy offers a high bound for the fading margin, approximating to the simulation curves for low and high bandwidths.

5. Conclusions

The statistical characterization of the channels IEEE 802.15.3a and IEEE 805.4a has been revised in this paper. We showed that UWB channels with small scale fading statistics modeled as lognormal RV can be approximated in the frequency domain by a Nakagami-m distribution, whose fading and mean power parameters are explicit functions of the delay parameters and decay time constants of the UWB channel. We also found the exact expression for the correlation coefficient between a couple of subcarriers amplitudes in frequency for the IEEE 802.15.3a UWB channel. Additionally, we also obtained analytical expressions of the fade depth and fading margin for the UWB channel energy IEEE 802.15.4a as a function of the frequency and different channels (i.e., narrowband, wideband and ultra wideband).

References

[1] FCC, "First report and order in the matter of revision of Part 15 of the Commission's rules regarding ultra-wideband transmission systems," ET-Docket 98-153 FCC, 02-48, pp. 12, Adopted: Feb. 14, 2002; released: Apr. 22, 2002.

[2] A.F. Molisch, "Ultra wideband propagation channels theory, measurement, and modeling," IEEE Trans. on Veh. Technol., vol. 54, pp. 1528-1545, Sep. 2005.

[3] European Committee for Standardization. (2007, Apr.). Standardization mandate forwarded to cen/cenelec/etsi for harmonised standards covering ultra-wideband equipment. [Online]. Available: http://www.etsi.org/WebSite/document/aboutETSI/EC_Mandates/m407_EN_Adonis_13099.pdf

[4] J. R. Foerster et al., "Channel modeling subcommittee final report," IEEE, Document IEEE 02490r0P802-15 SG3a, 2003.

[5] A.F. Molish et al,. "IEEE 802.15.4a channel model final report," Tech. Rep., Document IEEE 802.1504-0062-02-004a, 2005.

[6] A.M. Saleh and R. Valenzuela, "A statistical model for indoor multipath propagation," IEEE J. Select. Areas Commun, vol. 2, pp. 128-137, Feb. 1987.

[7] H. Hashemi, "Impulse response modeling of indoor radio propagation channels," IEEE J. Select. Areas Commun., vol. 11, pp. 967–978, Sep. 1993.

[8] M. Nakagami, "The m-distribution, a general formula of intensity distribution of rapid fading," in Statistical Methods of Radio Wave Propagation, W. G. Hoffman, Ed. Oxford, England: Pergamon 1960.

[9] M. Abramowitz and I. A. Stegun, Handbook of Mathematical Functions; with Formulas, Graphs and Mathematical Tables. New York: Dover, 1972.

[10] W.Q. Malik, B. Allen, and D.J. Edwards, "Bandwidth dependent modeling of small scale fade depth in wireless channel," in IET Microw. Antennas Propag., vol. 2, pp. 519-528, 2008.

[11] WolframMathworld. (2009, Jan). [Online]. Available: http://functions.wolfram.com/GammaBetaErf/InverseGammaRegularized.

Biographies

Gonzalo Llano R, was born in Cali, Colombia, He received his M.S.degree in Technologies, Systems and Communications Networks from Technical University of Valencia (Spain) in 2007. He is currently a Ph. D. student and researcher at the Radio and Wireless Communications Group (RWCG) in the iTEAM Research Institute at the Technical University of Valencia. His research is focused on modeling and statistical characterization of UWB channels, adaptive modulation systems with multicarrier transmission for UWB (MB-OFDM UWB), security and quality of services in WPAN networks with UWB.

Fade depth and fading margin have an asymptotic convergence for channel bandwidths beyond 1.5 GHz.

Juan Reig was born in Alcoy, Spain, in 1969. He received the M.S. and Ph.D. degrees in Telecommunications Engineering from the Technical University of Valencia, Spain, in 1993 and 2000, respectively. He has been a faculty member in the Department of Communications at the Technical University of Valencia, Spain since 1994, where he is now Associate Professor of Telecommunication Engineering. He is a member of the Radio and Wireless Communications Group (RWCG) of the Telecommunications and Multimedia Applications Research Institute (iTEAM). His areas of interest include fading theory, diversity, ultra-wide band systems and vehicular communications in V2V and V2I networks.

Lorenzo Rubio received the Telecommunication Engineering and the Ph. D degrees from the Universidad Politécnica de Valencia (UPV), Spain, in 1996 and 2004 respectively. In 1996, he joined the Communications Department of the UPV, where he is now Associate Professor of wireless communications. He is a member of the Radio and Wireless Communications Group (RWCG) of the Telecommunications and Multimedia Applications Research Institute (iTEAM). His main research interests ar related to wireless communications. Specific current research topics include radiowave propagation, measurement and mobile time-varying channels modelling in vehicular applications, ultra-wideband (UWB) communication systems, MIMO systems and equalization techniques in digital wireless systems. Dr. Rubio was awarded by the Ericsson Mobile Communications Prize from the Spanish Telecommunications Engineer Association for his study on urban statistical radiochannels characterisation applied to wireless communications.

Alexis Paolo García Ariza was born in Bucaramanga, Colombia, He received his M.S. degree in Electronic Engineering from the Industrial University of Santander (UIS), Bucaramanga, Colombia, in 2002. He is a Ph.D. candidate at the Universidad Politécnica de Valencia (UPV), where he was with the support of the European AlBan Programme from 2004 to 2008. He was with RadioGIS research group at UIS between 2002 and 2004. He was also a Research Engineer at the iTEAM Research Institute at UPV between 2004 and 2008. He is currently a Research Assistant at the Electronic Measurement Research Lab, Institute of Information Technology, Ilmenau University of Technology, Ilmenau, Germany.

His research areas are wireless channel characterization, propagation modeling, and mobile network planning tools. Currently he is focused on modelling, simulation and measurement/sounding of wireless channels, i.e., wideband MIMO channels, ultra-wideband (UWB) channels, and millimetre-wave (MM-Wave) channels applied to in-flight entertainment systems.